Materials Chemistry and Physics 134 (2012) 549–554

Contents lists available at SciVerse ScienceDirect

Materials Chemistry and Physics

journal homepage: www.elsevier.com/locate/matchemphys

Role of metal ions of Langmuir–Blodgett film in hydrophobic to hydrophilic transition of HF-treated Si surface

J.K. Bal [a,*,1], Sarathi Kundu [b], S. Hazra [a]

[a] Surface Physics Division, Saha Institute of Nuclear Physics, 1/AF Bidhannagar, Kolkata 700064, India
[b] Physical Sciences Division, Institute of Advanced Study in Science and Technology, Vigyan Path, Paschim Boragaon, Garchuk, Guwahati, Assam 781035, India

ARTICLE INFO

Article history:
Received 28 July 2011
Received in revised form 10 February 2012
Accepted 7 March 2012

Keywords:
X-ray reflectivity
Interfaces
Thin films
X-ray photoelectron spectroscopy (XPS)

ABSTRACT

Hydrophobic to hydrophilic transition of HF-treated Si surface strongly depends upon the metal ions, which are present in the headgroups of the deposited Langmuir–Blodgett (LB) film. Structure of LB films studied by X-ray reflectivity technique and chemical analysis of LB film–substrate interfaces studied by X-ray photoelectron spectroscopy combinedly suggest that the partial transition or partial oxidation of the HF-treated Si surface takes place under the subphase water but further transition or oxidation is possible only in the presence of metal ions. Electrovalent and covalent natures of the metal ions tune this transition or oxidation. Ni ions, for which bonding with headgroups are electrovalent in nature, are favorable for such transition/oxidation and as a result, complete transition/oxidation takes place when nickel arachidate LB film is deposited. On the other hand, Cd ions, for which bonding with headgroups show covalent nature, is not favorable for such transition and can not oxidize the underlying H-passivated Si substrate totally when cadmium arachidate LB film is deposited on such HF-treated Si surface. This ion-specific hydrophobic to hydrophilic transition is visualized by X-ray reflectivity, contact angle and X-ray photoelectron spectroscopy measurements.

1. Introduction

Semiconductor specially Si, due to its importance in the electronics industry like micro and opto-electronic devices, memory chips [1,2], and biological sensors [3,4], is perhaps the mostly investigated electrode material. The stability of such surface in air is highly desirable from the application point of view because such passivation minimizes the surface electronic density of states by terminating the surface dangling bonds [5].

Wet chemical passivation of the surface is the best way to restore a surface contamination free in the ambient conditions [6–8]. Different wet chemical passivations are there namely H- [9], Br- [10,11], Cl- [11–13], I-passivation [14], etc. Among these the most effective and stable passivation is the H-passivation [15–17]. The stability of such passivated surface is different in different environments [18–22]. Humidity of air [23–25], oxygen content in air or dissolved oxygen in water [26–28] and metal impurity [29–32] on the passivated surface play crucial role in stability or instability of the surface. With time native oxide will try to grow on the surface by desorbing the H-atom [15,16]. It is well known that H-passivated Si surface is hydrophobic in nature and the surface covered with native oxide by replacing the H-atom is hydrophilic in nature [17]. By studying the growth of the amphiphilic molecules in LB technique [33–35] it is possible to give an idea about the hydrophobicity or hydrophilicity of the surface and from that it is also possible to extract the information about the oxide coverage on the surface [17]. The advantage of structural study of LB film does not lies only in finding the nature of the surface but it can also act as a passivation layer where oxide layer cannot be used [11].

In our previous study [21], at the time of the growth of nickel arachidate (NiA) LB film on HF-treated Si surface, i.e., on H-passivated Si surface, a partial hydrophilic transition took place under the subphase water and as a result we obtained both asymmetric monolayer (AML, i.e., molecules in asymmetric configuration with hydrophilic head in one side and hydrophobic tails in other side) and symmetric monolayer (SML, i.e., molecules in symmetric configuration with head in the middle and hydrocarbon tails in both sides) structures. Presence of AML and SML suggests the hydrophilicity and hydrophobicity of the surface, respectively. Such transition was not completed under the high pH water subphase even after sufficient time of immersion because we have got SML structure of appreciable amount. It was completed after the attachment of Ni bearing headgroups with substrate surface. The formation of only AML/SML structure (SML structure sits on the AML) in further deposition confirms the complete transition. Attached Ni bearing headgroups in AML structure of NiA LB film

* Corresponding author. Tel.: +91 9474168964.
E-mail address: jayanta.bal@gmail.com (J.K. Bal).
[1] Present address: Centre for Advanced Materials, Indian Association for the Cultivation of Science, Kolkata 700032, India.

0254-0584/$ – see front matter © 2012 Elsevier B.V. All rights reserved.
doi:10.1016/j.matchemphys.2012.03.033

weaken the underlying Si–Si covalent bonds and easily oxidize the surface, which is hydrophilic in nature. Electrostatic interaction of Ni ions with the ligands was responsible for such reactions. Now the question is that if we replace Ni ions with Cd ions in the headgroup, which interact covalently (i.e., strongly) with the arachidic acid headgroups [36] to form better ordered CdA Langmuir monolayer, then will it affect the hydrophobic to hydrophilic transition of the HF-treated Si substrate?

In this article, by using X-ray reflectivity (XRR), X-ray photoelectron spectroscopy (XPS) and contact angle measurement techniques we have investigated the hydrophobic to hydrophilic transition of the HF-treated Si surface at the time of CdA LB film growth. The structure of this film obtained from the detail XRR data analysis and chemical nature of the surface/interface obtained from XPS analysis are compared with that of the NiA LB film [21] in order to find out the role of the metal ions of LB films for such hydrophobic to hydrophilic transition.

2. Experimental

Arachidic acid [$CH_3(CH_2)_{18}COOH$, Sigma, 99%] molecules were spread from a 0.5 mg ml^{-1} chloroform (Aldrich, 99%) solution on Milli-Q water (resistivity 18.2 MΩ cm) containing cadmium chloride ($CdCl_2 \cdot 2H_2O$, Merck, 99%) in a Langmuir trough (Apex Instruments). The pH of the water subphase containing 0.2 mM cadmium chloride was maintained at 8.5–9.0 using sodium hydroxide (NaOH, Merck, 98%). No buffers were used to maintain the pH of the subphase. Nearly 8 h were spent for pH stabilization including initial magnetic stirring. Prior to deposition, surface pressure-specific molecular area ($\pi - A$) isotherm of CdA Langmuir monolayer on water surface was recorded. π was measured with a Wilhelmy plate and the monolayer was compressed at a constant rate of 3 mm min^{-1}. All depositions were done at π = 30 mN m^{-1} and at room temperature (22 °C). Depositions were carried out at a speed of 2 mm min^{-1} and the drying time allowed after each up stroke was 10 min.

Prior to the LB film deposition, Si(0 0 1) substrates were made H-passivated by keeping it in hydrofluoric acid (HF, Merck, 10%) for 3 min at room temperature (22 °C) after ultrasonic cleaning in trichloroethylene (10 min) and methanol (10 min) solution. In the final step of HF-treatment, immediately after taken out from the HF solution all the substrates were kept inside the Milli-Q water for nearly 2 min and substrates were labeled as H–Si. LB films on H–Si substrates were deposited using different numbers of down and/or up strokes of substrates through Langmuir monolayers. One CdA LB film was deposited by 1 (up) stroke and another by 3 (up-down-up) strokes, referred as 1s-CdA/H–Si and 3s-CdA/H–Si, respectively. It should be mentioned here that Langmuir monolayers were allowed to deposit on H–Si substrate when π becomes 30 mN m^{-1} and for that it took ~40 min after spreading of the molecules on water surface. During this time period H–Si substrates were kept under the subphase water as the LB film depositions took place in odd number of strokes, which start with upstroke sequence.

XRR measurements were carried out using a versatile X-ray diffractometer (VXRD) setup to investigate the structure of LB films prepared in different strokes on HF-treated Si(0 0 1) substrates. VXRD consists of a diffractometer (D8 Discover, Bruker AXS) with Cu source (sealed tube) followed by a Göbel mirror to select and enhance Cu Kα radiation (λ = 1.54 Å). The diffractometer has a two-circle goniometer (θ–2θ) with quarter-circle Eulerian cradle as sample stage. The latter has two circular (χ and ϕ) and three translational (X, Y, and Z) motions. Scattered beam was detected using NaI scintillation (point) detector. Data were taken in specular condition, i.e., the incident angle (θ) is equal to the reflected angle (θ) and both are in a scattering plane. Under such condition, a non-vanishing wave vector component, q_z, is given by $(4\pi/\lambda)\sin\theta$ with resolution 0.0014 Å^{-1}. XRR technique essentially provides an electron density profile (EDP), i.e., in-plane (x–y) average electron density (ρ) as a function of depth (z) in high resolution [15]. From EDP it is possible to estimate film thickness, electron density, and interfacial roughness. Analysis of XRR data has been carried out using Parratt's formalism [37]. In this formalism the reflectivity as a function of q_z for a thin film of finite thickness d over a substrate, is given as $R(q_z) = rr^*$, where

$$r = \frac{r_{12} + r_{23}}{1 + r_{12}r_{23}} \tag{1}$$

with r_{12} and r_{23} being the reflectance for the vacuum–film and film–substrate interfaces, respectively. The above calculation can be extended for n such thin stratified layers of thickness d and one arrives at a recursive formula in terms of Fresnel reflectance given by

$$r^F_{n-1,n} = \frac{r_{n,n+1} + F_{n-1,n}}{1 + r_{n,n+1}F_{n-1,n}} e^{(-iq_{z,n-1}d_{n-1})} \tag{2}$$

where

$$F_{n-1,n} = \frac{q_{z,n+1} - q_{z,n}}{q_{z,n+1} + q_{z,n}} \tag{3}$$

In the nth stratified layer the corresponding wave vector is defined as $q_{z,n} = (q_z^2 - q_{c,n}^2)^{1/2}$. The Fresnel reflectance for the interface between nth and $(n-1)$th stratified layer is modified to include the roughness σ_n of the nth stratified layer and one can finally write the reflectance of a rough surface as

$$r_{n-1,n} = r^F_{n-1,n} e^{(-(1/2)iq_{z,n-1}q_{z,n}\sigma^2)} \tag{4}$$

In general, the electron-density variation in a specimen is determined by assuming a model and comparing the simulated profile with the experimental data. EDP is extracted from the fitting of experimental XRR data.

Contact angle measurements were carried out to verify the hydrophilic or hydrophobic nature of the Si substrate after immersion into different solutions (e.g., HF and $CdCl_2$ solution). Chemical nature of such Si surfaces and also after LB film deposition was investigated by XPS measurements. XPS measurements were performed with an Omicron Multiprobe (Omicron NanoTechnology) spectrometer fitted with an EA125 hemispherical analyzer and a monochromatized Al Kα (1486.6 eV) source.

3. Results and discussion

3.1. X-ray reflectivity and electron-density profile

LB films consist of amphiphilic molecules where hydrophilic head and hydrophobic tail are present. In case of arachidic acid, the tail part ended up with non-polar CH_3 group whereas the head part consists of polar COOH group. In the subphase water, incorporation of metal ions into the head part in place of H atom facilitates the transfer of molecules from the water subphase to the substrate surface in order to form a good LB film [35]. Depending upon the nature of the substrate surface LB film follows the favorable structure, i.e., it attaches with the substrate through head (AML) for hydrophilic surface and through tail (SML) for hydrophobic surface [17]. As the XRR technique provides EDP along depth, it is possible to find out the structure (AML or SML, etc.) of the LB film. By knowing this structure one can get an idea about the hydrophilic/hydrophobic nature of the substrate surface.

XRR data and analyzed curves of 1s-CdA/H–Si and 3s-CdA/H–Si samples are shown in Fig. 1a and b, respectively. Just to compare these profiles with that of the CdA films grown on the freshly oxide covered hydrophilic surface (labeled as 1s-CdA/OH–Si and 3s-CdA/OH–Si), we have plotted their XRR profiles in Fig. 1c and d,

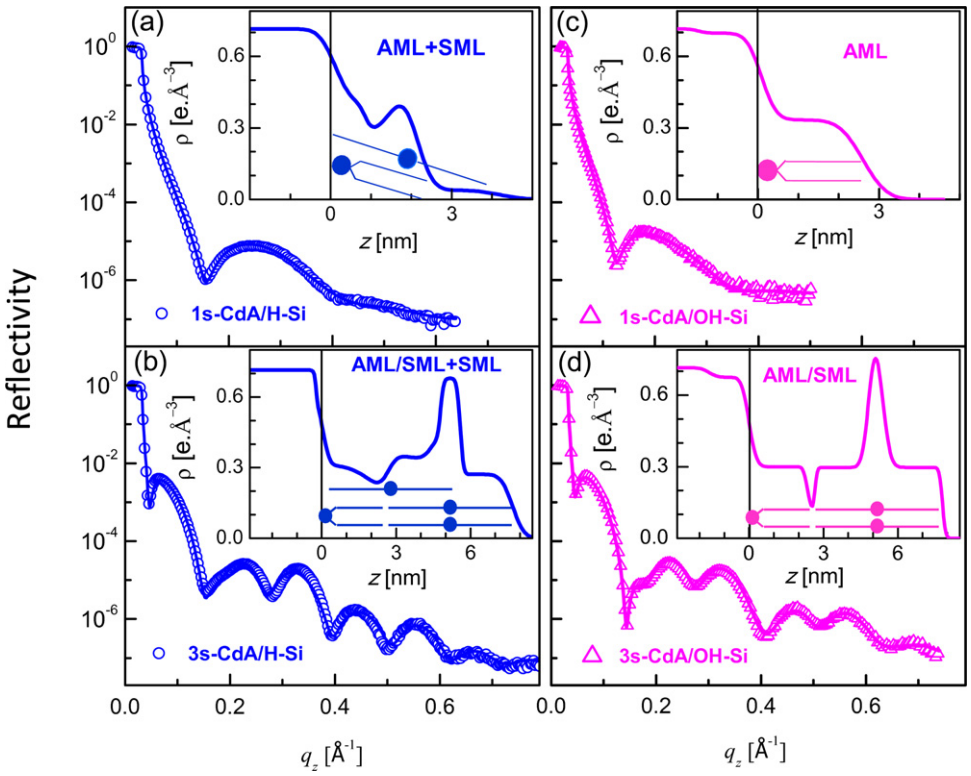

Fig. 1. XRR data (different symbols) and analyzed curves (solid line) of CdA LB films deposited on H-passivated Si surfaces by (a) one stroke, (b) three strokes and on OH-passivated Si surfaces by (c) one stroke and (d) three strokes. Insets: corresponding EDP and cartoon of the structure.

respectively. The XRR profiles of 1s-CdA/OH–Si and 3s-CdA/OH–Si samples (shown in Fig. 1c and d) are different from that of 1s-CdA/H–Si (shown in Fig. 1a) and 3s-CdA/H–Si sample (shown in Fig. 1b), respectively. To get the quantitative information about the structure and structural differences all the XRR data has been fitted with considering a model structure and corresponding EDPs are given in their insets. EDP of 1s-CdA/H–Si sample suggests that the film mainly consists of AML structure along with few SML, which are schematically presented in the inset of Fig. 1a. The high density peak at $Z \sim 1.7$ nm above from the interface position, which is due to the presence of metal (Cd) into the head part of LB film, and thickness of the film ~4.5 nm combinely suggest the existence of SML structure. The very low uniform electron density above the peak is coming from the hydrocarbon tail part. The electron density below the peak is much greater than the above, which is the indicative of the existence of some other structure whose thickness should be ~2 nm. It suggests the presence of AML structure. Although the density below the peak is not uniform, which is the indicative of imperfect structures [33], probably very few molecules are randomly oriented in this region. In case of only AML structure as obtained in 1s-CdA/OH–Si sample (shown in Fig. 1c) the high density (~0.74 e Å^{-3}) head of small thickness (~0.5 nm) could not be observed as it is directly attached with the high density (~0.715 e Å^{-3}) Si substrate. It reveals as a roughness of the Si substrate. For 3s-CdA/H–Si sample, EDP (shown in Fig. 1b) shows that the film consists of mostly AML/SML along with few SML (cartoons are shown in the inset of Fig. 1b). The presence of head (peak in EDP of Fig. 1b) at $Z \sim 5$ nm above from the interface with uniform low electron density in either direction confirms the presence of SML structure on the top of AML. The dip in EDP (at $Z \sim 2.3$ nm) observed at the AML-SML junction due to presence of low density H atom at the end of the tail. If only AML/SML structure is present as obtained in 3s-CdA/OH–Si sample (shown in Fig. 1d) the electron density of the tails should be nearly same. But in 3s-CdA/H–Si sample, the electron density of the lower tail (below the head) is greater than that of the top tail (above the head). It suggests the presence another structure likely to be SML along with the AML/SML. From the EDPs (shown in Fig. 1a and b) we have roughly quantified the individual contributions of each structure. From the ρ value of the tail part it is possible to get an idea about the coverages of constituent structures assuming the maximum tail density 0.33 e Å^{-3} as 100% coverage. For 1s-CdA/H–Si sample, the uniform low density layer above the hump (shown in the inset of Fig. 1a) is nothing but the tail part of SML structure. The ρ value of the tail is 0.045 e Å^{-3}. Thus the coverage of the SML structure is ~14%, while rest of the amount, i.e., 86% is of the AML assuming full coverage of the LB film. Similarly for 3s-CdA/H–Si sample, the ρ value of the top tail part, which is only the contribution of AML/SML structure (shown in Fig. 1b), is 0.27 e Å^{-3}. Thus, the coverage of AML/SML structure is ~82%. As the density of the lower part below the high density metal bearing head region is almost reaching the maximum value, thus essentially the coverage of SML should be ~18%. These suggest that the SML coverage is nearly same for both the sample, while the remaining portion is covered with AML structure for the 1s-CdA/H–Si sample and with AML/SML structure for the 3s-CdA/H–Si sample. The small difference in the amount of constituent structures (i.e., AML or AML/SML and SML) for two samples may arise due to the error in the estimation as those structures are not exactly perfect [33]. In our previous study [21] we have seen that NiA LB film takes both AML and SML structure of nearly equal amount (i.e., 50%) in one stroke and only AML/SML structure in three strokes on H–Si surface. Thus, in one stroke the SML amount is much greater for NiA film compared to that of CdA film.

3.2. Contact angle measurement

The wettability of the H–Si surface before and after immersion into the $CdCl_2$ solution is investigated by contact angle

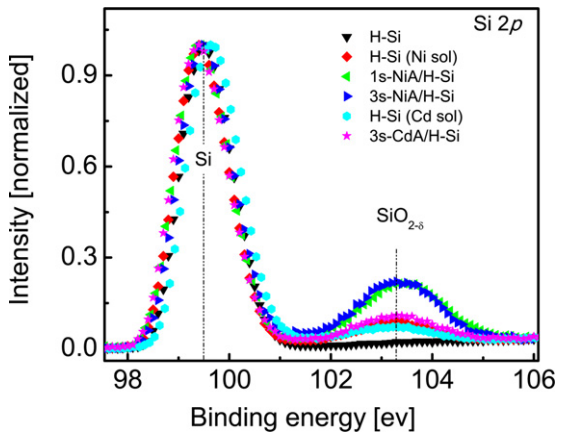

Fig. 2. XPS spectra of six different samples in the Si 2p binding energy region. Two peaks appear due to substrate (Si) and surface or interfacial oxide layer ($SiO_{2-\delta}$), are indicated.

measurement. The contact angle of water with the H–Si surface is ∼79° [21]. After immersion into $CdCl_2$ solution during 40 min [substrate is labeled as H–Si(Cd sol)] the contact angle reduces to 25-28°. The RCA cleaned Si, which is known to the complete hydrophilic surface, makes 14°-17° contact angle with the water drop [21]. These suggest that due to the immersion into the $CdCl_2$ solution the hydrophobic H–Si surface becomes nearly hydrophilic.

3.3. X-ray photoelectron spectroscopy

The Si 2p core-level spectra of H–Si, H–Si(Cd sol) and 3s-CdA/H–Si samples are shown in Fig. 2. For the first two samples, XPS measurements were done just after the preparation, whereas for third sample it was done after XRR measurements, which took nearly 2 h. The peak at ∼99.5 eV represents Si^0 chemical state while that at ∼103.4 eV represents Si^{4+} chemical state, corresponding to silicon (Si) substrate and silicon oxide ($SiO_{2-\delta}$) layer, respectively. The data presented in Fig. 2 is the normalized data with respect to the Si^0 peak intensity. The oxide layer is completely absent in the H–Si surface as can be seen in Fig. 2. After immersion into the $CdCl_2$ solution, resulting substrate known as H–Si(Cd sol), the surface is partially oxidized. For 3s-CdA/H–Si sample, $SiO_{2-\delta}$ peak intensity is slightly greater than that of H–Si(Cd sol) sample. As the former sample is placed in the environment for longer time (∼2 h) before entering into XPS chamber in order to do XRR measurement, the amount of oxidation may be greater. To compare with the NiA film we have also plotted the XPS data of H–Si(Ni sol) (i.e., here sol indicates $NiSO_4$ solution), 1s-NiA/H–Si and 3s-NiA/H–Si samples, which are taken from our previous study [21]. The oxidation of the H–Si(Ni sol) substrate after the immersion into $NiSO_4$ solution is similar to that of H–Si(Cd sol) substrate. In solution, the oxidation is mainly triggered by the pH of the solution as the oxidation mechanism starts with the replacement of H by hydroxyl ion (OH^-) [21]. Probably very few metal ions (e.g., Cd^{2+}, Ni^{2+}) that may physisorbed on the surface could not oxidize appreciably and accordingly no significant difference in the $SiO_{2-\delta}$ peak intensity for H–Si(Cd sol) and H–Si(Ni sol) samples (shown in Fig. 2) is observed. But there was a significant increment in the oxidation after the attachment of NiA LB film, unlike to CdA LB film, with the substrate, i.e., in 1s-NiA/H–Si and 3s-NiA/H–Si samples as clearly evident in Fig. 2. In this case the presence of metal ions in the headgroup of LB film is significant and plays strong role in further oxidation.

3.4. Mechanism of hydrophobic to hydrophilic transition

In 1s-CdA/H–Si sample presence of very few SML structure along with the AML suggests that hydrophobic spots are still present on the surface. For 3s-CdA/H–Si sample, the SML coverage is nearly similar to that of in 1s-CdA/H–Si sample, which is expected. Rest of the region is covered by AML/SML structured LB film. This indicates that the partial hydrophilic transition takes place under subphase water (shown in Fig. 3). Also the contact angle measurements well support this partial transition. Such hydrophilicity arises due to the rapid oxidation of the HF-treated Si surface under high pH subphase water, which is clearly evident from Fig. 2. The hydroxyl ion (OH^-) replaced the H-atom in order to form silanol group (Si–OH). Due to strong electronegativity of OH^- groups, Si–SiOH back bond is weakened and is attacked by rest of the OH^- ions. The Si–H bond is quickly replaced by OH^- ion. Now the two such neighboring silanol group face each other and oxide is formed through a bridging reaction of these groups [21]. This partial transition is also observed in our previous study [21] where $NiSO_4$ salt was dissolved into the subphase water (shown in Fig. 3). The contact angle of water after immersing into the $CdCl_2$ solution(∼25–28°) is slightly less than that into the $NiSO_4$ solution (∼34°). This may be due to the small difference in pH, which plays significant role in partial transition as mentioned before, of two solutions. It is highly possible that the pH of $CdCl_2$ solution are slightly more than that of $NiSO_4$ solution as it is very difficult to have two solutions having exactly the same pH value.

It should be mentioned here that the coverage of SML structure in 1s-CdA/H–Si sample is much less than that of in 1s-NiA/H–Si sample though there is not much difference in hydrophilicity or hydrophobicity (from the contact angle measurements). It is well known that the growth of LB film is strongly related to the structure or order of the starting Langmuir monolayer, which can be tuned through the selection of different metal ions such as Cd, Ni, etc., having different type and/or strength of interaction [36]. Ni ions interact electrostatically (i.e., less strongly) with arachidic acid headgroups to form NiA Langmuir monolayer, whereas Cd ions interact covalently (i.e., strongly) with arachidic acid headgroups to form better ordered CdA Langmuir monolayer. As a result, CdA molecules show that they are coupled and cannot flip easily, while NiA molecules show that they are flexible enough and can flip easily from AML to SML structure near the hydrophilic–hydrophobic domain boundary and then diffuse from hydrophilic to nearby hydrophobic portion of Si surface during single stroke of deposition [17].

On the other hand, after the attachment of CdA LB film with the H–Si surface no significant increment of the hydrophilicity (shown in Fig. 3), i.e., increment of AML/SML percentage (shown in Fig. 1b) and the oxide amount (shown in Fig. 2) is not observed. It is known that the presence of some metals like Ni [32], Na [31], Bi [29], Cu [30], etc., on the Si surface can create instability and as a result Si surface easily oxidized at ambient condition. This is due to the underlying bond weakening in presence of those metals. Such metals (also metal ions) are present freely on the surface. Whereas in our previous study [21], we observed that though the Ni ions electrostatically bonded in the head of NiA LB film, it can weaken the Si–Si underlying bond in order to form native oxide layer. Such oxidation also strongly depends on the amount of Ni ion in the headgroup that can be varied by changing the pH of the subphase solution. The oxide growth rate increases with the amount of Ni ion in the headgroup. Due to the oxidation after NiA LB film attachment the H–Si substrate surface becomes completely hydrophilic and in further deposition ultimately forms AML/SML structure (shown in Fig. 3). The ionic nature of the Ni–carboxylic ligand bonding helps to do that. The covalent nature of the Cd–carboxylic ligand

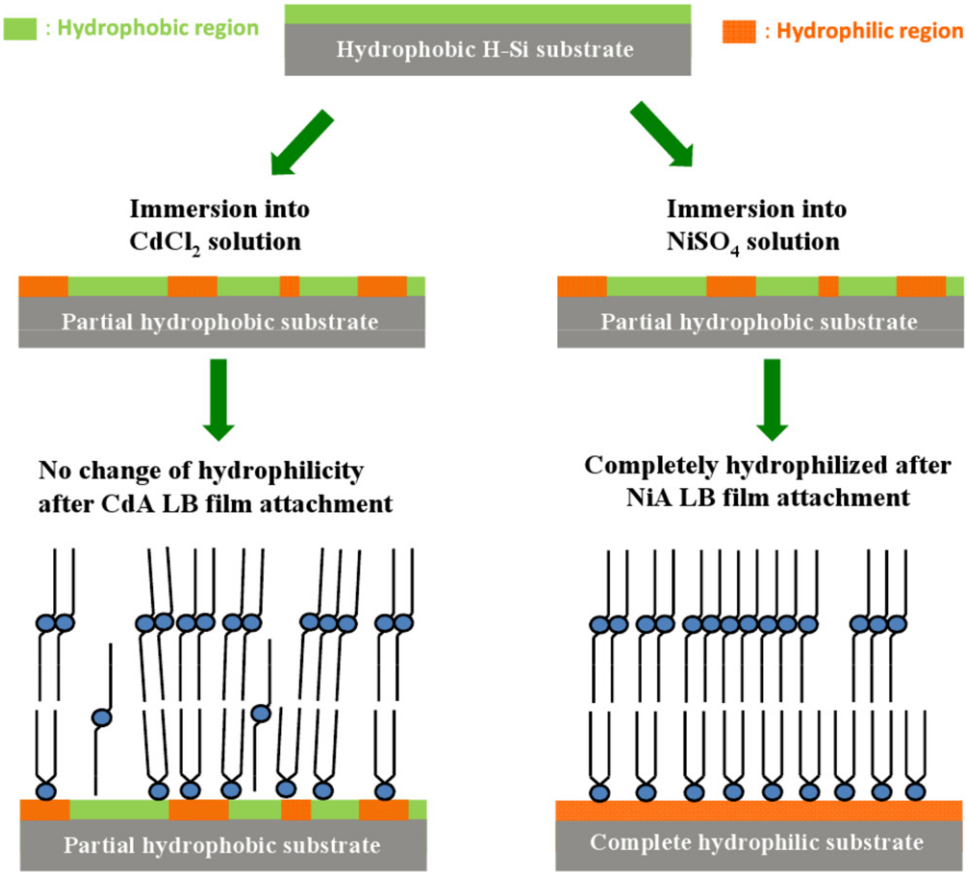

Fig. 3. Schematics of the ion-specific hydrophobic to hydrophilic (partial or complete) transition of H–Si surface.

bonding [36] could not weaken the underlying Si–Si bonds in order to oxidize the Si surface. The advantage of using CdA LB film on H–Si surface is that it does not react with the substrate surface and can be used as a passivating layer of Si surface.

4. Conclusion

The structural analysis of CdA LB film deposited on HF-treated Si surface by using X-ray reflectivity technique suggests that complete hydrophobic to partial hydrophobic or hydrophilic transition of HF-treated Si surface takes place under the $CdCl_2$ solution similar to under the $NiSO_4$ solution. Such transition is well explained considering the strong role of OH^- ion-induced oxide growth. After the attachment of CdA LB film no further oxidation and accordingly no complete hydrophilic transition take place unlike the NiA LB film. The Cd ion, present in the headgroup of LB film, could not oxidize the underlying Si substrate where as Ni ion easily oxidizes it. Covalent nature of Cd mainly inhibit in doing this.

Acknowledgments

Authors would like to thank Mr. A.K.M. Maidul Islam and Prof. M. Mukherjee for their help in XPS measurements and Prof. S. Banerjee and Ms. A. Bhattacharya for their help in contact angle measurements. S. Kundu acknowledges Prof. A. K. Raychaudhuri for his support to access LB trough facility and financial support from Department of Science and Technology.

References

[1] M. Tabe, Y. Yamamoto, Appl. Phys. Lett. 69 (1996) 2222–2224.
[2] K. Morimoto, K. Araki, K. Yamashita, K. Morita, M. Niwa, Appl. Surf. Sci. 117–118 (1997) 652–659.
[3] M.G. Nikolaides, S. Rauschenbach, S. Luber, K. Buchholz, M. Tornow, G. Abstreiter, A.R. Bausch, Chemphyschem 4 (2003) 1104–1106.
[4] F. Tao, G.Q. Xu, Acc. Chem. Res. 37 (2004) 882–893.
[5] V. Derycke, P.G. Soukiassian, F. Amy, Y.J. Chabal, M.D. D'Angelo, H.B. Enriquez, M.G. Silly, Nat. Mater. 2 (2003) 253–258.
[6] H. Ubara, T. Imura, A. Hiraki, Solid State Commun. 50 (1984) 673–675.
[7] E. Yablonovitch, D.L. Allara, C.C. Chang, T. Gmitter, T.B. Bright, Phys. Rev. Lett. 57 (1986) 249–252.
[8] V.A. Burrows, Y.J. Chabal, G.S. Higashi, K. Raghavachari, S.B. Christman, Appl. Phys. Lett. 53 (1988) 998–1000.
[9] G.W. Trucks, K. Raghavachari, G.S. Higashi, Y.J. Chabal, Phys. Rev. Lett. 65 (1990) 504–507.
[10] K. Sekar, P.V. Satyam, G. Kuri, D.P. Mahapatra, B.N. Dev, Nucl. Instrum. Methods Phys. Res. B 71 (1992) 308–313.
[11] J. Terry, R. Mo, C. Wigren, R. Cao, G. Mount, P. Pianetta, M.R. Linford, C.E.D. Chidsey, Nucl. Instrum. Methods Phys. Res. B 133 (1992) 94–101.
[12] C.-Y. Ruan, V.A. Lobastov, F. Vigliotti, S. Chen, A.H. Zewail, Science 304 (2004) 80–84.
[13] P.L. Silvestrelli, F. Toigo, F. Ancilotto, J. Phys. Chem. B 110 (2006) 12022–12028.
[14] C.H. Lee, Z.D. Lin, N.G. Shang, L.S. Liao, I. Bello, N. Wang, S.T. Lee, Phys. Rev. B 62 (2000) 17134–17137.
[15] J.K. Bal, S. Hazra, Phys. Rev. B 75 (2007), 205411-1–6.
[16] J.K. Bal, S. Hazra, Phys. Rev. B 79 (2009), 155412-1–6.
[17] J.K. Bal, S. Kundu, S. Hazra, Phys. Rev. B 81 (2010), 045404-1–8.
[18] X. Zhang, E. Garfunkel, Y.J. Chabal, S.B. Christman, E.E. Chaban, Appl. Phys. Lett. 79 (2001) 4051–4053.
[19] S. Rivillon, F. Amy, Y.J. Chabal, M.M. Frank, Appl. Phys. Lett. 85 (2004) 2583–2585.
[20] M. Dai, Y. Wang, J. Kwon, M.D. Halls, Y.J. Chabal, Nat. Mater. 8 (2009) 825–830.
[21] J.K. Bal, S. Kundu, S. Hazra, Chem. Phys. Lett. 500 (2010) 90–95.
[22] X.G. Zhang, Electrochemistry of Silicon and Its Oxide, Kluwer Academic Publishers, New York, 2004.
[23] M. Niwano, J. Kageyama, K. Kurita, K. Kinashi, I. Takahashi, N. Mlyamoto, J. Appl. Phys. 76 (1994) 2157–2164.
[24] T. Ohmi, J. Electrochem. Soc. 143 (1996) 2957–2964.
[25] E.S. Snow, G.G. Jernigan, P.M. Cambell, Appl. Phys. Lett. 76 (2000) 1782–1784.
[26] Y.J. Chabal, S.B. Christman, Phys. Rev. B 29 (1984) 6974–6976.

[27] M. Ranke, Y.R. Xing, Surf. Sci. 157 (1985) 339–352.
[28] E. Kondoh, M.R. Baklanov, F. Jonckx, K. Maex, Mater. Sci. Semicond. Process. 1 (1998) 107–117.
[29] T. Hanada, M. Kawai, Vacuum 41 (1990) 650–651.
[30] D. Graf, M. Grundner, D. Muhlhoff, M. Dellith, J. Appl. Phys. 69 (1991) 7620–7626.
[31] S. Xu, P. Xu, M. Ji, X. Liu, M. Ma, J. Zhu, Y. Zhang, J. Mater. Sci. Technol. 9 (1993) 437–440.
[32] N. Takano, N. Hosoda, T. Yamada, T. Osaka, Electrochim. Acta 44 (1999) 3743–3749.
[33] S. Hazra, A. Gibaud, A. Desert, V. Gacem, N. Cowlam, Physica B 283 (2000) 45–48.
[34] K.B. Blodgett, I. Langmuir, Phys. Rev. 51 (1937) 964–982.
[35] M.C. Petty, Langmuir–Blodgett films, An Introduction, Cambridge University Press, New York, 1996.
[36] W. Dong, R. Wang, G. Mao, H. Möhwald, Soft Matter 2 (2006) 686–692.
[37] L.G. Parratt, Phys. Rev. 95 (1954) 359–369.